

Article

Solvent-Induced Unsymmetric Salamo-Like Trinuclear Ni^{II} Complexes: Syntheses, Crystal Structures, Fluorescent and Magnetic Properties

Jing Li ¹, Hong-Jia Zhang ¹, Jian Chang ¹, Hao-Ran Jia ¹, Yin-Xia Sun ^{1,*}  and Yong-Qing Huang ²

¹ School of Chemical and Biological Engineering, Lanzhou Jiaotong University, Lanzhou 730070, China; iclijing1@163.com (J.L.); zhj020809@163.com (H.-J.Z.); chemdennis@163.com (J.C.); jiahr12@163.com (H.-R.J.)

² State Key Laboratory of Mining Disaster Prevention and Control Co-founded by Shandong Province and the Ministry of Science and Technology, College of Chemical and Environmental Engineering, Shandong University of Science and Technology, Qingdao 266590, China; yquang3@163.com

* Correspondence: sun_yinxia@163.com

Received: 26 March 2018; Accepted: 16 April 2018; Published: 18 April 2018



Abstract: Solvent-induced trinuclear Ni^{II} complexes, $[\{\text{Ni}(\text{L})(\text{MeOH})\}_2(\text{OAc})_2\text{Ni}] \cdot 2\text{MeOH}$ (**1**), $[\{\text{Ni}(\text{L})(\text{EtOH})\}_2(\text{OAc})_2\text{Ni}] \cdot 2\text{H}_2\text{O}$ (**2**), $[\{\text{Ni}(\text{L})(n\text{-PrOH})\}_2(\text{OAc})_2\text{Ni}] \cdot 2\text{H}_2\text{O}$ (**3**) and $[\{\text{Ni}(\text{L})(i\text{-PrOH})\}_2(\text{OAc})_2\text{Ni}]$ (**4**), have been prepared with an unsymmetric Salamo-like ligand H₂L, and characterized via X-ray crystallography, FT-IR, UV-Vis and fluorescence spectra. In complexes **1**, **2**, **3** and **4**, there are two ligand (L)²⁻ moieties, two acetato ligands, two coordinated methanol, ethanol, *n*-propanol or *i*-propanol molecules, respectively, as well as other crystallizing solvent molecules. Two acetato ligands coordinated to the three Ni^{II} ions via usual Ni-O-C-O-Ni bridges, and four μ -phenoxo oxygen atoms coming from two [NiL(solvent)] units coordinate to the central Ni^{II} ions. Although different solvents are induced in the complexes, all the Ni^{II} ions are six-coordinated and adopt geometries of distorted octahedron. Magnetic measurements were performed on complex **2**, an intramolecular antiferromagnetic interaction was observed between Ni^{II} ions and a simulation of the experimental data gives $J = -2.96 \text{ cm}^{-1}$ and $g = 2.30$.

Keywords: unsymmetric Salamo-like ligand; Ni^{II} complex; crystal structure; fluorescence spectroscopy; magnetic property

1. Introduction

Metal complexes bearing Salen-like ligands or their derivatives are now a significant research subject [1–15], and could be of ubiquitous use in biological systems [16–24], fluorescent sensors [25–37], magnetic properties [38–42], optical materials [43–51] and building blocks for supramolecular features [52–62]. Though a number of advances have been obtained in the researches of Salen-like Ni^{II} complexes [63–69], there might be novel applications for such a group of unique compounds. Compared with the symmetric Salen-like ligands, the unsymmetric Salen-like ligands are uncommon because electronic and steric effects of unsymmetric configurations with Salen-like ligands or their derivatives would provide more structural changes and coordination compounds [70–75] and would be expected to acquire new features [76]. In addition, the construction of complexes is often affected by many subtle factors such as ligands, metal ions, solvents, pH values and temperatures [42,77–80]. Among them (except for ligands), the solvents are perhaps also clear and direct factors [81–83]. In order to research the structural features, spectral characteristics, magnetic properties and investigated solvent effects of the transition metal complexes with unsymmetric Salen-like ligands, we herein study four supramolecular Ni^{II} complexes **1**, **2**, **3** and **4** with a new unsymmetric Salamo-like ligand.

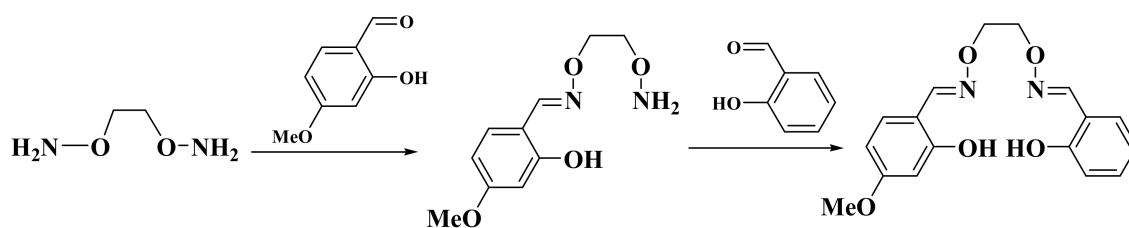
2. Experimental

2.1. Material and General Methods

All chemicals were used without further purification, and were of analytical reagent grades. C, H, and N analyses were acquired by an Elementar GmbH VarioEL V3.00 automatic elemental analysis instrument (Hanau, Germany). Elemental analyses for Ni^{II} ions were detected by an IRIS ER/S-WP-1 ICP atomic emission spectrometer (Elementar, Berlin, Germany). Keep accounts of the IR spectra data using the VERTEX70 FT-IR spectrophotometer (Bruker, Karlsruhe, Germany), and the samples were prepared as KBr (500–4000 cm⁻¹) pellets. ¹H NMR spectra were recorded using a Mercury-400BB spectrometer (Varian, Palo Alto, CA, USA) at 400 MHz. Melting points were measured via an X₄ microscopic melting point apparatus produced by Beijing Taiké Instrument Limited Company (Beijing, China) and were uncorrected. Fluorescent spectra were performed on a LS-55 fluorescence photometer (Perkin-Elmer, Norwalk, America). X-ray single crystal structure determinations were performed on a Bruker Smart Apex CCD diffractometer (Karlsruhe, Germany). Magnetic susceptibility data were measured on powdered samples of complex **2** using a Quantum Design model MPMS XL7 SQUID magnetometer (Quantum Design, San Diego, CA, America). Magnetic susceptibility measurements were performed at 1000 Oe in the 2–300 K temperature range.

2.2. Synthesis of H₂L

1,2-Bis(aminoxy)ethane and 4-methoxy-2,2'-[ethylenediylldioxybis(nitrilomethylidyne)]diphenol (H₂L) were prepared on the basis of a similar procedure [84–88]. Synthetic route to the ligand is depicted in Scheme 1. Yield: 48%. M.p.: 69–71 °C. ¹H NMR (400 MHz, CDCl₃): δ: 3.81 (s, 3H, CH₃), 4.44 (m, 4H, CH₂), 6.46–6.49 (m, 2H, ArH), 6.89–6.92 (d, *J* = 12 Hz, 1H, ArH), 6.97–6.99 (d, *J* = 8 Hz, 1H, ArH), 7.04–7.06 (d, *J* = 8 Hz, 1H, ArH), 7.15–7.17 (d, *J* = 8 Hz, 1H, ArH), 8.18 (s, 1H, CH=N), 8.24 (s, 1H, CH=N), 9.75 (s, 1H, OH), 9.92 (s, 1H, OH). Anal. Calcd. for C₁₇H₁₈N₂O₅ (%): C, 61.81; H, 5.49; N, 8.48; Found (%): C, 62.05; H, 5.52; N, 8.38.



Scheme 1. The synthetic route to H₂L.

2.3. Syntheses of Ni^{II} Complexes **1**, **2**, **3** and **4**

Complex 1: A pale-green methanol solution (2 mL) of Ni^{II} acetate tetrahydrates (3.81 mg, 0.015 mmol) was added dropwise to a colorless acetonitrile solution (2 mL) of H₂L (3.23 mg, 0.01 mmol). The solution color was pale-green still. The mixed solution was filtered, and the filtrate was placed at room temperature to slowly evaporate; about two weeks later, light green block crystals suitable for single crystal X-ray diffraction were gained. Anal. Calcd. for C₄₂H₅₄Ni₃N₄O₁₈ (%): C, 46.75; H, 5.04; N, 5.19; Ni, 16.32. Found (%): C, 46.97; H, 5.16; N, 5.02; Ni, 16.13.

Complex 2: Complex **2** was prepared by a method similar to that of complex **1** except substituting methanol with ethanol and acetonitrile with acetone. The color of the mixture continued to be pale-green but cooled off immediately and clear light green, block-like crystals were gained after two weeks following the solvent was slowly evaporated. Anal. Calcd. for C₄₀H₄₆Ni₃N₄O₂₀ (%): C, 44.53; H, 4.30; N, 5.19; Ni, 16.32. Found (%): C, 44.68; H, 4.45; N, 5.01; Ni, 16.15.

Complex 3: Complex 3 was prepared by changing methanol to n-propanol and acetonitrile to dichloromethane. The color of the mixture continued to be pale-green but cooled off immediately and clear light green, block-like crystals were gained after one week. Anal. Calcd. for $C_{44}H_{58}Ni_3N_4O_{18}$ (%): C, 47.74; H, 5.28; N, 5.06; Ni, 15.91. Found (%): C, 47.89; H, 5.35; N, 4.92; Ni, 16.07.

Complex 4: Complex 4 was prepared by changing methanol to isopropanol and acetonitrile to dichloromethane. The color of the mixture continued to be pale-green but cooled off immediately and clear light green, block-like crystals were gained after ten days. Anal. Calcd. for $C_{44}H_{50}Ni_3N_4O_{16}$ (%): C, 49.53; H, 4.72; N, 5.25; Ni, 16.50. Found (%): C, 49.75; H, 4.88; N, 5.13; Ni, 16.26.

2.4. X-ray Crystallography

Because of the similar structures of the complexes 1–4, only the details of the data collection and refinements of Ni^{II} complex 1 are presented in Table 1 (That of 2, 3 and 4 are listed in Table S1). A single crystal of Ni^{II} complexes 1, 2, 3 and 4 was put on a Bruker Smart 1000 CCD area detector. The reflections were collected by a graphite monochromated Mo $K\alpha$ radiation ($\lambda = 0.71073 \text{ \AA}$) at 294K for Ni^{II} complexes 1, 2 and 4, and that of Ni^{II} complex 3 was collected by a graphite monochromated Cu $K\alpha$ radiation ($\lambda = 1.54184 \text{ \AA}$) at 293 K. The structures were solved by the program SHELXL-97 and Fourier difference techniques, and were refined by the full-matrix least-squares method on F^2 . All hydrogen atoms were added in calculated positions. The non-hydrogen atoms were refined anisotropically. Supplementary crystallographic data for this paper have been deposited at Cambridge Crystallographic Data Centre (1480197, 1480194, 1480196 and 1480195 for complexes 1, 2, 3 and 4) and can be gained free of charge via www.ccdc.cam.ac.uk/conts/retrieving.html.

Table 1. Crystal data and structure refinements for Ni^{II} complex 1.

Molecular Formula	$C_{42}H_{54}Ni_3N_4O_{18}$	Molecular Weight	1079.02
Temperature (K)	294.29 (10)	Crystal Size, mm^3	$0.36 \times 0.24 \times 0.21$
Crystal System	tetragonal	Space Group	$I4_1/a$
A (\AA)	30.0337 (6)	α ($^\circ$)	90
B (\AA)	30.0337 (6)	β ($^\circ$)	90
C (\AA)	11.4332 (4)	γ ($^\circ$)	90
V (\AA^3)	10312.9 (5)	Z	8
D_{calc} (Mg/m^3)	1.390	μ (mm^{-1})	1.155
F(000)	4496	hkl Range	$-40 \leq h \leq 37, -22 \leq k \leq 40, -15 \leq l \leq 8$
Θ Range ($^\circ$)	3.3–26.0	Reflections Collected/Unique	14,913/5038
Rint	0.0538	Data/Restraints/Parameters	5038/17/312
R_1/wR_2 [$I \geq 2\sigma(I)$]	0.0606/0.1649	R_1/wR_2 (All Data)	0.0970/0.1842
Goodness Off It (GOF)	1.086	$\Delta\rho_{max,min}$ ($e \text{ \AA}^{-3}$)	0.97/−0.37

3. Results and Discussion

H_2L is white powder, stable in air and soluble in some organic solvents such as ethanol, methanol, CH_2Cl_2 , $CHCl_3$, acetonitrile, acetone, DMF and THF, but insoluble in Et_2O , n-hexane. Ni^{II} complexes 1, 2, 3 and 4 are all soluble in $CHCl_3$ and DMF, but not soluble in n-hexane, Et_2O , acetone and acetonitrile.

3.1. Crystal Structure Descriptions of Ni^{II} Complexes 1, 2, 3 and 4

Selected bond lengths and angles for Ni^{II} complexes 1, 2, 3 and 4 are listed in Table 2. Crystal structures and atom numberings of complexes 1, 2, 3 and 4 are depicted in Figures 1–4, respectively.

X-ray crystal structure analyses revealed that the Ni^{II} complexes 1, 2, 3 and 4 take on similar crystal structures, which all are symmetric trinuclear structures. The crystals of Ni^{II} complexes are solved as tetragonal space group $I4_1/a$ (1), triclinic space group $P-1$ (2), monoclinic space group $C2/c$ (3) and monoclinic space group $P2_1/n$ (4), respectively. All the Ni^{II} complexes consist of three Ni^{II} ions, two $(L)^{2-}$ moieties, two μ -acetato ligands, and two coordinated methanol, ethanol, n-propanol or i-propanol molecules in Ni^{II} complexes 1, 2, 3 and 4, respectively, as well as crystalizing solvent molecules (two MeOH in 1 and two H_2O in 2 and 3, respectively).

Table 2. Selected bond lengths (Å) and angles (°) for Ni^{II} complexes **1**, **2**, **3** and **4**.

Complex 1		Complex 2		Complex 3		Complex 4	
Bond	Distance	Bond	Distance	Bond	Distance	Bond	Distance
Ni1-O1	2.013(3)	Ni1-O1	2.009(3)	Ni1-O1	2.025(2)	Ni1-O1	1.994(3)
Ni1-O4	2.037(3)	Ni1-O4	2.007(3)	Ni1-O4	2.011(2)	Ni1-O4	1.999(3)
Ni1-O6	2.121(3)	Ni1-O6	2.126(3)	Ni1-O6	2.118(3)	Ni1-O6	2.352(4)
Ni1-O7	2.033(3)	Ni1-O7	2.045(3)	Ni1-O7	2.019(3)	Ni1-O7	2.045(4)
Ni1-N1	2.079(4)	Ni1-N1	2.029(4)	Ni1-N1	2.077(3)	Ni1-N2	2.030(5)
Ni1-N2	2.073(4)	Ni1-N2	2.050(4)	Ni1-N2	2.078(3)	Ni1-N1	2.053(5)
Ni2-O1	2.064(3)	Ni2-O1	2.100(3)	Ni2-O1	2.077(2)	Ni2-O1	2.094(3)
Ni2-O1 #1	2.064(3)	Ni2-O1 #2	2.100(3)	Ni2-O1 #3	2.077(2)	Ni2-O1 #4	2.094(3)
Ni2-O4	2.086(3)	Ni2-O4 #2	2.085(3)	Ni2-O4	2.063(2)	Ni2-O4	2.074(3)
Ni2-O4 #1	2.086(3)	Ni2-O4	2.085(3)	Ni2-O4 #3	2.063(2)	Ni2-O4 #4	2.074(3)
Ni2-O8	2.091(3)	Ni2-O8	2.065(3)	Ni2-O8	2.096(2)	Ni2-O8	2.019(3)
Ni2-O8 #1	2.091(3)	Ni2-O8 #2	2.065(3)	Ni2-O8 #3	2.096(2)	Ni2-O8 #4	2.019(3)
Bond	Angle	Bond	Angle	Bond	Angle	Bond	Angle
O1-Ni1-O4	79.56(13)	O1-Ni1-O6	89.93(12)	O1-Ni1-O6	90.41(10)	O1-Ni1-O4	85.73(12)
O1-Ni1-O6	87.46(13)	O1-Ni1-O7	90.97(13)	O1-Ni1-N1	86.81(10)	O1-Ni1-O6	78.59(15)
O1-Ni1-O7	93.97(13)	O1-Ni1-N1	89.32(15)	O1-Ni1-N2	166.77(11)	O1-Ni1-O7	91.07(14)
O1-Ni1-N1	87.47(15)	O1-Ni1-N2	169.44(14)	O4-Ni1-O1	79.16(9)	O1-Ni1-N2	164.74(18)
O1-Ni1-N2	165.26(16)	O4-Ni1-O1	81.13(11)	O4-Ni1-O6	90.64(10)	O1-Ni1-N1	86.77(18)
O4-Ni1-O6	93.29(14)	O4-Ni1-O6	92.19(13)	O4-Ni1-O7	92.94(11)	O4-Ni1-O6	78.99(14)
O4-Ni1-N1	166.96(14)	O4-Ni1-O7	90.17(13)	O4-Ni1-N1	165.92(11)	O4-Ni1-O7	89.79(14)
O4-Ni1-N2	86.86(14)	O4-Ni1-N1	170.44(14)	O4-Ni1-N2	87.75(11)	O4-Ni1-N2	88.69(17)
O7-Ni1-O4	91.11(13)	O4-Ni1-N2	89.62(14)	O7-Ni1-O1	92.69(10)	O4-Ni1-N1	172.17(18)
O7-Ni1-O6	175.56(15)	O7-Ni1-O6	177.58(13)	O7-Ni1-O6	175.65(10)	O7-Ni1-O6	165.19(14)
O7-Ni1-N1	88.42(15)	O7-Ni1-N2	94.15(15)	O7-Ni1-N1	88.80(12)	O7-Ni1-N1	92.63(18)
O7-Ni1-N2	91.96(14)	N1-Ni1-O6	87.63(17)	O7-Ni1-N2	89.87(14)	N2-Ni1-O6	86.41(18)
N1-Ni1-O6	87.44(16)	N1-Ni1-O7	90.13(17)	N1-Ni1-O6	88.32(12)	N2-Ni1-O7	103.11(18)
N2-Ni1-O6	87.65(14)	N1-Ni1-N2	99.88(17)	N2-Ni1-N2	106.24(12)	N2-Ni1-N1	98.0(2)
N2-Ni1-N1	106.18(16)	N2-Ni1-O6	85.32(15)	N2-Ni2-O6	87.79(14)	N1-Ni1-O6	97.30(19)

Table 2. Cont.

Complex 1		Complex 2		Complex 3		Complex 4	
O1 #1-Ni2-O1	180.00(14)	O1-Ni2-O1 #2	180.0	O1 #3-Ni2-O1	180.0	O1-Ni2-O1 #4	180.0
O1-Ni2-O4	77.30(12) (12)12	O4 #2-Ni2-O1 #2	77.21(11)	O1 #3-Ni2-O8	91.16(9)	O4-Ni2-O1 #4	98.65(12)
O1 #1-Ni2-O4 #1	77.30(12)	O4-Ni2-O1	77.21(11)	O1 #3-Ni2-O8 #3	88.84(9)	O4-Ni2-O1	81.35(12)
O1-Ni2-O4 #1	102.70(12)	O4-Ni2-O1 #2	102.79(11)	O1-Ni2-O8	88.84(9)	O4 #4-Ni2-O1	98.65(12)
O1 #1-Ni2-O4	102.70(12) (12)12	O4 #2-Ni2-O1	102.79(11)	O1-Ni2-O8 #3	91.16(9)	O4 #4-Ni2-O1 #4	81.35(12)
O1-Ni2-O8 #1	90.85 (13)	O4-Ni2-O4 #2	180.00(9)	O4 #3-Ni2-O1	103.20(9)	O4 #4-Ni2-O4	180.0
O1 #1-Ni2-O8	90.85(13)	O8-Ni2-O1 #2	90.95(12)	O4 #3-Ni2-O1 #3	76.80(9)	O8-Ni2-O1 #4	90.07(13)
O1-Ni2-O8	89.15(13)	O8 #2-Ni2-O1	90.95(12)	O4-Ni2-O1 #3	103.20(9)	O8 #4-Ni2-O1 #4	89.93(13)
O1 #1-Ni2-O8 #1	89.15(13)	O8-Ni2-O1	89.05(12)	O4-Ni2-O1	76.80(9)	O8 #4-Ni2-O1	90.07(13)
O4 #1-Ni2-O4	180.0	O8 #2-Ni2-O1 #2	89.05(12)	O4-Ni2-O4 #3	180.0(9)	O8-Ni2-O1	89.93(13)
O4-Ni2-O8	89.39(12)	O8-Ni2-O4 #2	90.64(11)	O4-Ni2-O8 #3	90.64(9)	O8 #4-Ni2-O4	90.26(13)
O4 #1-Ni2-O8	90.61(12)	O8 #2-Ni2-O4 #2	89.36(11)	O4 #3-Ni2-O8 #3	89.36(9)	O8 #4-Ni2-O4 ¹	89.75(13)
O4 #1-Ni2-O8 #1	89.39(12)	O8-Ni2-O4	89.36(11)	O4-Ni2-O8	89.36(9)	O8-Ni2-O4 #4	90.25(13)
O4-Ni2-O8 #1	90.61(12)	O8 #2-Ni2-O4	90.64(11)	O4 #3-Ni2-O8	90.64(9)	O8-Ni2-O4	89.75(13)
O8 #1-Ni2-O8	180.0	O8-Ni2-O8 #2	180.00(15)	O8-Ni2-O8 #3	180.0	O8-Ni2-O8 #4	180.0

Symmetry transformations used to generate equivalent atoms: #1: $1 - x, 1 - y, -z$; #2: $1 - x, -y, 1 - z$; #3: $-x, 1 - y, 1 - z$ and #4: $2 - x, 2 - y, 1 - z$ for Ni^{II} complexes **1**, **2**, **3** and **4**, respectively.

In Ni^{II} complexes **1**, **2**, **3** and **4**, each of the terminal Ni1 ions sat in the *cis*-N₂O₂ cavity (N1, N2, O1 and O4) of the deprotonated (L)²⁻ moieties, and carboxylate O7 atom from the μ-acetato bridge and O6 atom from the different alcohol ligands coordinated to Ni1 in axial positions. So the environment of the terminal Ni^{II} ion could be best described as an octahedral topology with the six-coordinated. Furthermore, the coordination environment of the central Ni2 ion is composed of four μ-phenoxo oxygen (O1, O4, O1[#] and O4[#]) atoms from two (L)²⁻ moieties and two μ-acetato oxygen (O8 and O8[#]) atoms which adopt a usual μ-O-C-O fashion. Four oxygen (O1, O4, O1[#] and O4[#]) atoms form the basal plane, and two oxygen (O8 and O8[#]) atoms situated in the axial positions; all the six oxygen atoms bind to Ni2 forming an octahedral configuration. Consequently, all the six-coordinated Ni^{II} ions of complexes **1**, **2**, **3** and **4** have a slightly distorted octahedral coordination polyhedron.

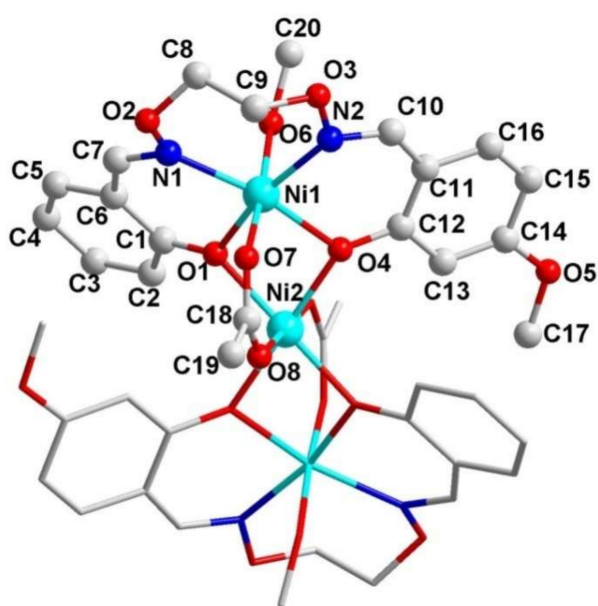


Figure 1. Molecular structure of complex 1.

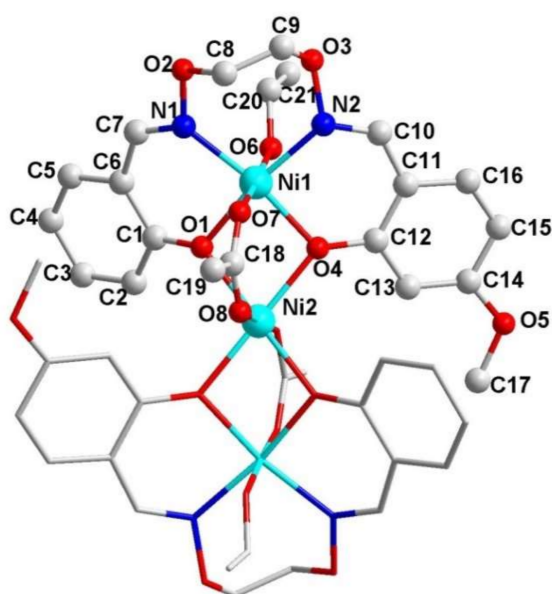


Figure 2. Molecular structure of complex 2.

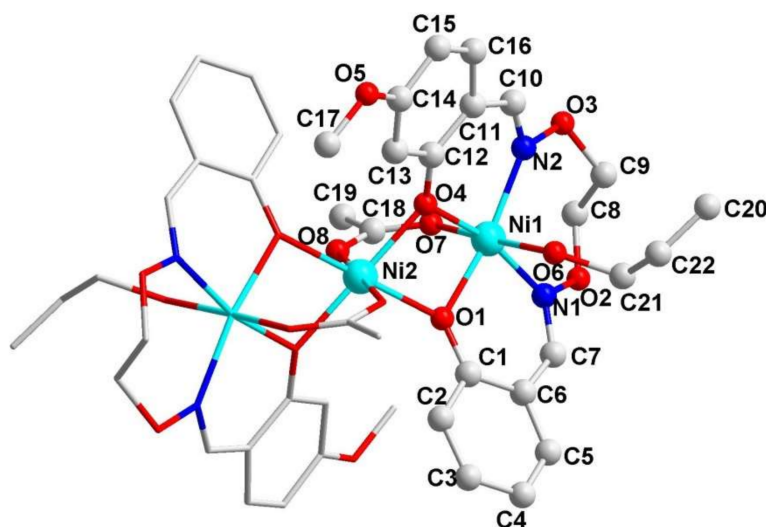


Figure 3. Molecular structure of complex 3.

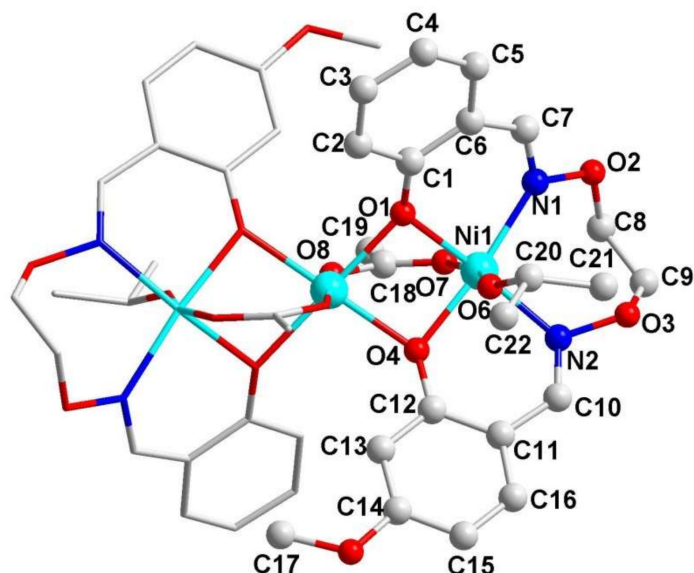


Figure 4. Molecular structure of complex 4.

Supramolecular Interactions of Ni^{II} Complexes 1, 2, 3 and 4

The molecular structures of Ni^{II} complexes 1, 2, 3 and 4 are similar to each other, but because of the intra- and inter-molecular hydrogen bond interactions (Table 3), their supramolecular structures are different. As depicted in Figure 5, in Ni^{II} complex 1, two pairs of intra-molecular C9-H9B...O7 and C2-H2...O8 hydrogen bonds are formed. The proton (-C2H2) of benzene rings of the (L)²⁻ moiety is hydrogen-bonded to the O8 atom of the acetato ligand. The proton (-C9H9B) of ethylenedioxiime carbons (C9) of the (L)²⁻ units is hydrogen-bonded to the O7 atom of the acetato ligand, and two pairs of inter-molecular O6-H6...O9 and O9-H9...O8 hydrogen bonds are formed. The proton (-O6H6) of the methanol molecules is hydrogen-bonded to the O9 atom of the methanol molecule. The proton (-O9H9) of the methanol molecule is hydrogen-bonded to the O8 atom of the acetato ligand.

In complex 2, two pairs of intra-molecular C8-H8A...O7 and C20-H20B...O3 hydrogen bonds are formed. The proton (-C8H8A) of ethylenedioxiime carbons (C8) of the (L)²⁻ units is hydrogen-bonded to the O7 atom of the acetato ligand. The proton (-C20H20B) of the ethanol molecule

is hydrogen-bonded to the O3 atom of ethylenedioxiime. As depicted in Figure 6, two pairs of inter-molecular O6-H6...O9 and O9-H9B...O8 hydrogen bonds are formed. The proton (-O6H6) of the ethanol molecule is hydrogen-bonded to the O9 atom of the H₂O molecule. The proton (-O9H9) of the H₂O molecule is hydrogen-bonded to the O8 atom of the acetato ligand.

Table 3. Intra- and inter-molecular hydrogen bonds (Å, °) for complexes 1, 2, 3 and 4.

Complex	D-H...A	d(D-H)	d(H...A)	d(D...A)	∠DHA
1	C9-H9B...O7	0.97	2.39	3.242(6)	147
	C2-H2...O8	0.93	2.56	3.243(7)	130
	O6-H6...O9	0.86(3)	1.76(3)	2.614(7)	176(3)
	O9-H9...O8	0.82	1.93	2.731(7)	165
2	C8-H8A...O7	0.97	2.18	3.088(8)	156
	O20-20B...O3	0.97	2.49	3.277(12)	139
	O6-H6...O9	0.87(4)	1.77(4)	2.626(8)	169(5)
	O9-H9B...O8	0.85	1.86	2.700(7)	171
3	C2-H2...O8	0.93	2.58	3.205(5)	125
	C8-H8A...O7	0.97	2.43	3.240(7)	140
	C13-H13...O8	0.93	2.55	3.219(5)	129
	O6-H6A...O9	0.86(5)	1.81(5)	2.643(4)	161(4)
	O6-H6B...O9	0.86(4)	1.82(4)	2.643(4)	161(7)
	O9-H9D...O8	0.86(4)	1.96(8)	2.712(5)	146(8)
4	C8-H8B...O7	0.97	2.22	3.134(9)	156
	C13-H13...O1	0.93	2.41	3.195(6)	142

As depicted in Figure 7, three pairs of intramolecular C2-H2...O8, C8-H8A...O7 and C13-H13...O8 hydrogen bonds are formed. The proton (-C2H2) of benzene rings of the (L)²⁻ moiety is hydrogen-bonded to the O8 atom of the acetato ligand. The O7 atom of the acetato ligand is hydrogen-bonded to the C8H8A group of ethylenedioxiime. The proton (-C13H13) of benzene rings of the (L)²⁻ moiety is hydrogen-bonded to the O8 atom of the acetato ligand, and three pairs of inter-molecular O6-H6A...O9, O6-H6B...O9 and O9-H9D...O8 hydrogen bonds are formed. The proton (-O6H6A and -O6H6B) of propanol is hydrogen-bonded to the O9 atom of the H₂O molecule. The proton (-O9H9D) of the H₂O molecule is hydrogen-bonded to the O8 atom of the acetato ligand.

As depicted in Figure 8, two pairs of intra-molecular C8-H8B...O7 and C13-H13...O1 hydrogen bonds are formed. The proton (-C8H8B) of ethylenedioxiime carbons is hydrogen-bonded to the O7 atom of the acetato ligand. The proton (-C13H13) of benzene rings of the (L)²⁻ moiety is hydrogen-bonded to the phenolic O1 atom.

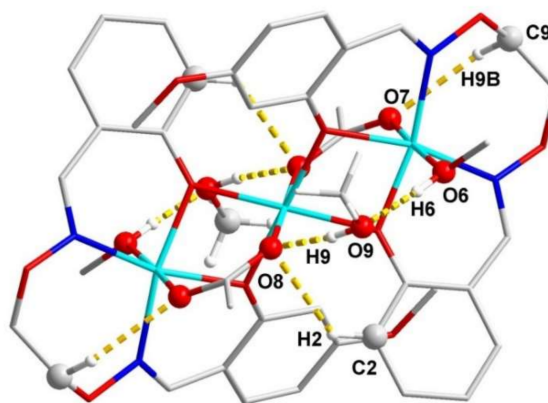


Figure 5. Intra- and inter-molecular hydrogen bonds of Ni^{II} complex 1.

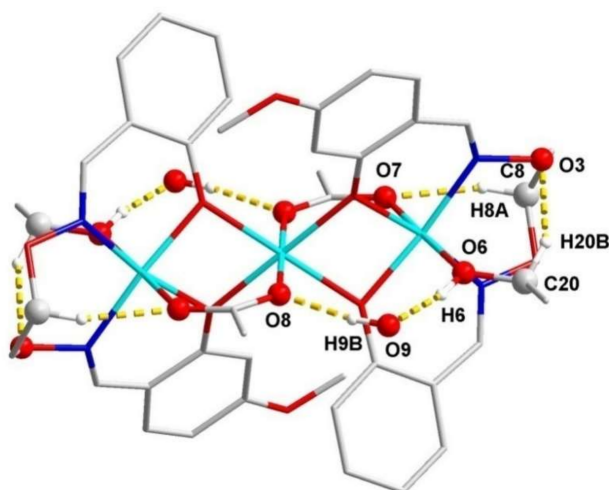


Figure 6. Intra- and inter-molecular hydrogen bonds of Ni^{II} complex 2.

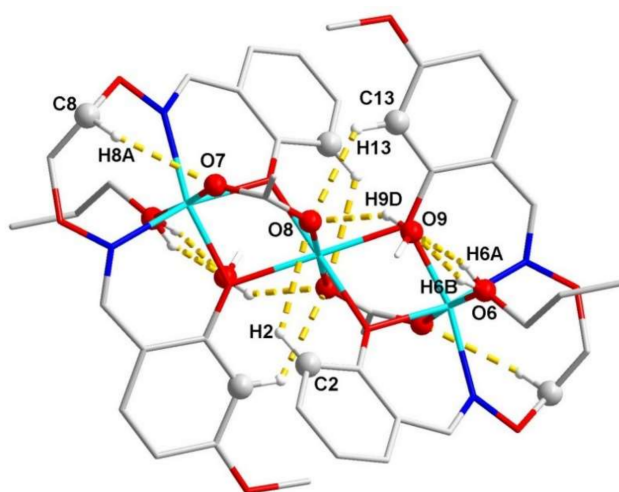


Figure 7. Intramolecular hydrogen bonds of Ni^{II} complex 3.

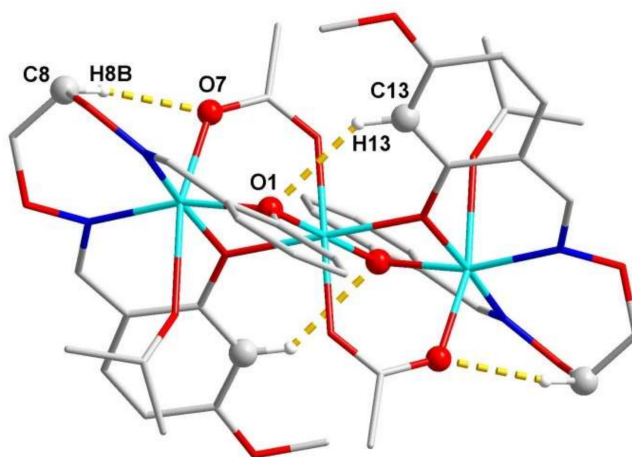


Figure 8. Intramolecular hydrogen bonds of the Ni^{II} complex 4.

3.2. IR Spectra

The IR spectra of H₂L and its corresponding Ni^{II} complexes **1**, **2**, **3** and **4** exhibited several distinguishable resonances in the region of 400–4000 cm⁻¹ and are depicted in Table 4 and Figure S1.

Table 4. Selected FT-IR data for H₂L and its Ni^{II} complexes **1**, **2**, **3** and **4** (cm⁻¹).

Compound	$\nu(\text{PhO-H})$	$\nu(\text{C=N})$	$\nu(\text{Ar-O})$	$\nu(\text{Ni-N})$	$\nu(\text{Ni-O})$
H ₂ L	3165	1632	1260		
Complex 1		1608	1219	588	420
Complex 2		1608	1217	592	410
Complex 3		1612	1219	592	409
Complex 4		1609	1215	590	419

The free ligand H₂L showed a broad typical O-H band at 3165 cm⁻¹. The vanishing of these bands in the FT-IR spectra of Ni^{II} complexes **1**, **2**, **3** and **4** indicated that the O-H groups of H₂L have been deprotonated and coordinated to the Ni^{II} ions [89]. The free ligand H₂L exhibited a typical C=N stretching band at 1632 cm⁻¹, which is moved to 1608, 1608, 1612 and 1609 cm⁻¹ in Ni^{II} complexes **1**, **2**, **3** and **4**, respectively, exhibiting a weak π -accepting ability of the deprotonated (L)²⁻ ligand [82]. The strong Ar-O stretching band within the 1263–1213 cm⁻¹ range always appears for the Salen-like ligands. This band occurred at 1260 cm⁻¹ for H₂L, and at 1219, 1217, 1219 and 1215 cm⁻¹ for Ni^{II} complexes **1**, **2**, **3** and **4**, respectively. The Ar-O stretching band is waved to lower frequency, exhibiting that Ni-O_(phenolic) bonds are formed in Ni^{II} complexes **1**, **2**, **3** and **4**.

The far-infrared spectra of Ni^{II} complexes **1**, **2**, **3** and **4** are gained in the region of 500–100 cm⁻¹ in order to identify Ni-N and Ni-O bonds. The spectrum showed $\nu(\text{Ni-N})$ and $\nu(\text{Ni-O})$ frequencies of Ni^{II} complex **1** at 588 and 420 cm⁻¹, Ni^{II} complex **2** at 592 and 410 cm⁻¹, Ni^{II} complex **3** at 592 and 409 cm⁻¹, and Ni^{II} complex **4** at 590 and 419 cm⁻¹, indicating that the Ni^{II} ions are bonded by N₂O₂ donor atoms of the (L)²⁻ moieties. Hence, it gives evidence for the coordination of H₂L with the Ni^{II} ions. These assignments are consistent with the literature frequency values [90].

3.3. UV-Vis Absorption Spectra

The UV-Vis spectra of H₂L and its Ni^{II} complexes **1**, **2**, **3** and **4** were determined in 1.0 × 10⁻⁵ mol · L⁻¹ ethanol solution (Figure 9). The spectrum of H₂L includes two relatively intense bands at 274 and 309 nm, attributed to the π - π^* transitions of the benzene rings in the salicylaldehyde and oxime groups [91]. Upon coordination of H₂L, the band at ca. 309 nm disappears, indicating that the oxime nitrogen atoms are coordinated to the Ni^{II} ions. The intraligand π - π^* transition of the benzene rings of salicylaldehyde is slightly waved, and appears at 278, 276, 277 and 279.5 nm in Ni^{II} complexes **1**, **2**, **3** and **4**, respectively. The new bands observed at 349, 348, 350 and 349 nm for Ni^{II} complexes **1**, **2**, **3** and **4**, respectively, are attributed to typical bands that are a result of mixing of L → M charge-transfer transitions with the d-d transitions of ³A_{2g} → ³T_{1g}(P) for octahedral Ni(II) ions, which are characteristic of transition metal N₂O₂ complexes and that of the spin-allowed d-d transition ³A_{2g} → ³T_{1g}(F) and the ³A_{2g} → ³T_{2g}(F) transition which usually appear after 600 nm.

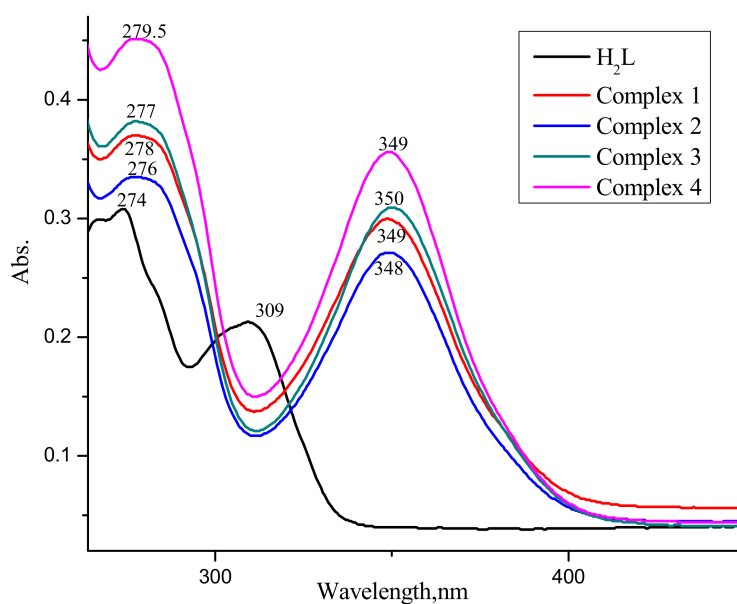


Figure 9. UV-Vis spectra of H_2L and its Ni^{II} complexes **1**, **2**, **3** and **4** in ethanol solution ($c = 1.0 \times 10^{-5} \text{ mol} \cdot \text{L}^{-1}$).

3.4. Fluorescence Properties

The emission spectra of H_2L and its Ni^{II} complexes in dilute ethanol solution ($c = 1.0 \times 10^{-5} \text{ mol} \cdot \text{L}^{-1}$) at room temperature are depicted in Figure 10. The ligand H_2L has no intense photoluminescence upon excitation at 350 nm. Ni^{II} complexes **1**, **2**, **3** and **4** showed photoluminescence with maximum emissions at ca. 407.9, 411.8, 415, 392.9 nm upon excitation at 350 nm, respectively. Ni^{II} complexes **1**, **2**, **3** and **4** showed intense photoluminescence which includes that fluorescence characteristics that have been affected by the introductions of the Ni^{II} ions.

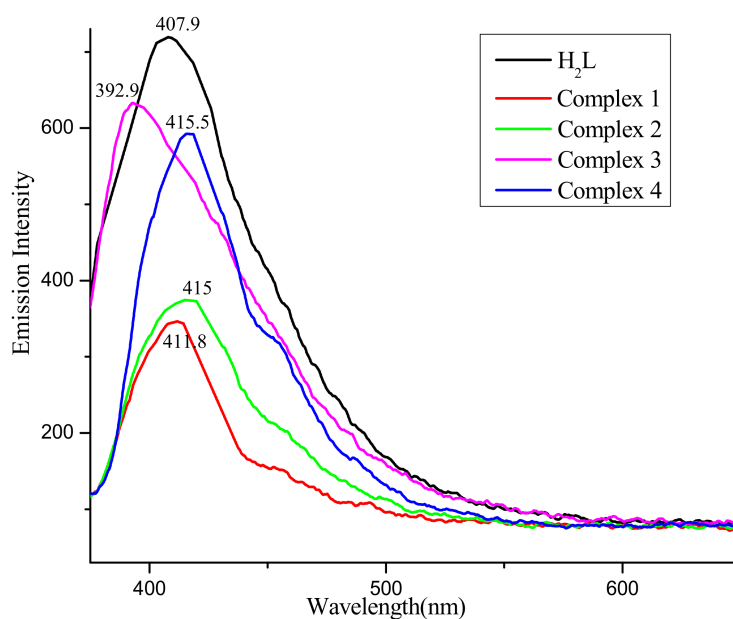


Figure 10. Emission spectra of Ni^{II} complexes **1**, **2**, **3** and **4** ($\lambda_{ex} = 350 \text{ nm}$) in ethanol solution ($c = 1 \times 10^{-5} \text{ mol} \cdot \text{L}^{-1}$).

3.5. Magnetic Properties

Because of the similar structure of the composites 1–4, there is little difference in their magnetic properties. Only the magnetic property of complex 2 is discussed. Magnetic analysis of complex 2 was measured under the applied magnetic field of 1000 Oe, and magnetic susceptibility data of complex 2 were measured within the 2–300 K temperature range. Samples were measured with the single crystals of complex 2. The temperature dependence of magnetic susceptibilities of Ni^{II} complex 2 is depicted in Figure 11, as a plot of $\chi_M T$ against T . The $\chi_M T$ value of $3.88 \text{ cm}^3 \cdot \text{K} \cdot \text{mol}^{-1}$ at 300 K for trinuclear Ni^{II} complex 2 is slightly higher than the value of $3.00 \text{ cm}^3 \cdot \text{K} \cdot \text{mol}^{-1}$ expected for three Ni^{II} ($3d^8, S = 1$) isolated ions. When decreasing the temperature, the $\chi_M T$ plot decreases very slowly till about 125 K and then begins to drop down sharply and reaches a minimum value of $0.58 \text{ cm}^3 \cdot \text{K} \cdot \text{mol}^{-1}$ at 2 K, suggesting that the dominant antiferromagnetic interactions are propagated between Ni^{II} ions. There is no peak in the χ_M vs. T plot. Therefore, no long-range magnetic ordering is found.

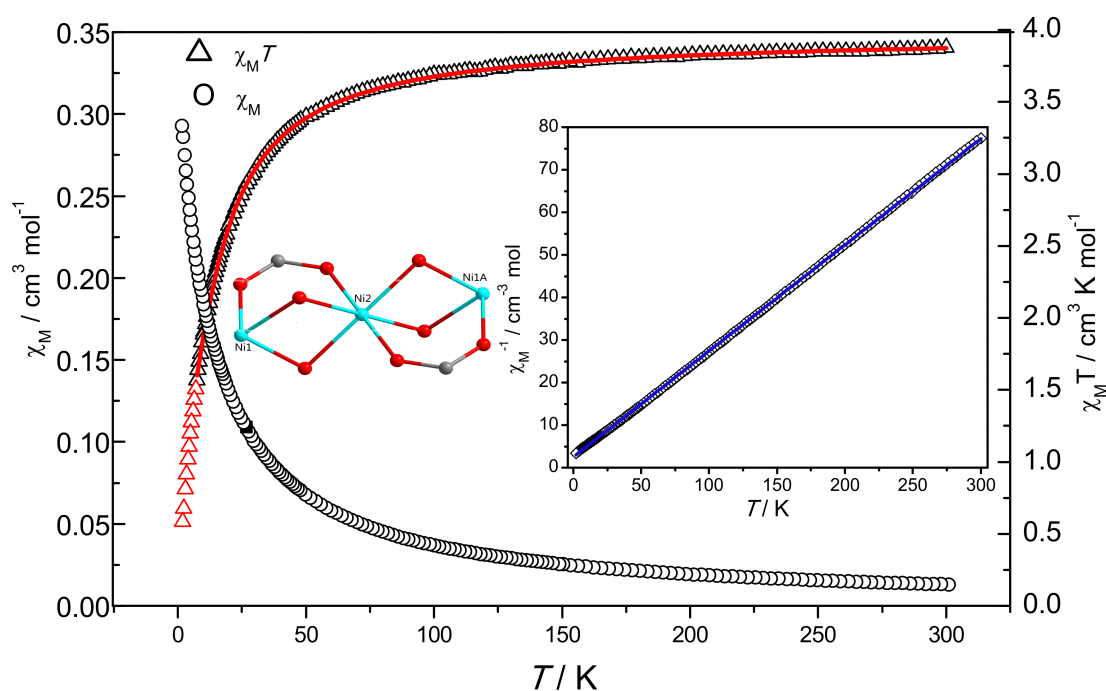


Figure 11. Temperature dependence of $\chi_M T$ and χ_M versus T of 2. Inset: temperature dependence of χ_M^{-1} ; the solid line represents the best fit of the Curie–Weiss law $\chi_M = C/(T - \theta)$.

The temperature dependence of the reciprocal susceptibility (χ_M^{-1}) follows the Curie–Weiss law ($\chi_M = C/(T - \theta)$) with a Weiss constant $\theta = -10.0549 \text{ K}$ and Curie constant $C = 4.0124 \text{ cm}^3 \cdot \text{K} \cdot \text{mol}^{-1}$ indicating a dominated intramolecular antiferromagnetic interaction. Inspection of the molecular structure reveals that one main exchange pathway exists in the interaction between Ni1...Ni2 by two $\mu_2\text{-O}$ (O1, O1A and O4, O4A). In order to analyze the experimental data of this linear antimagnetic ion core of Ni₃O₈ (Inset Figure 11), we tried to simulate the data by using the spin Hamiltonian $\hat{H} = -2J[(\hat{S}_1\hat{S}_2) + (\hat{S}_2\hat{S}_3)]$ to treat exchange interaction (J) between Ni^{II} ions, so the resulting magnetic susceptibility equation is:

$$\chi_M = \frac{2Ng^2\beta^2}{3kT} \left\{ \frac{A}{B} \right\}$$

$$A = 3x^{10} + 18x^6 + 3x^4 + 15x^2 + 42$$

$$B = 3x^{10} + x^8 + 8x^6 + 3x^4 + 5x^2 + 7$$

$$x = e^{-J/kT}$$

J is the intramolecular exchange integral between Ni^{II} ions, and the other symbols have their usual meanings. The best fitting for the experimental data of complex **2** gives $J = -2.96 \text{ cm}^{-1}$, $g = 2.30$ and the agreement factor $R = \sum[(\chi_{MT})_{obsd} - (\chi_{MT})_{calc}]^2 / \sum(\chi_{MT})_{obsd}^2$ is 2.51×10^{-4} . The small negative value of J also indicates that a weak antiferromagnetic interaction is operative between the Ni^{II} ions. The antiferromagnetic parameters of complex **2** are close to other Ni^{II} complex [92].

3.6. Solvent Effect

The structures revealed that the structural features of complexes **1**, **2**, **3** and **4** are found to be similar except for the distinction of coordinated and/or crystallizing solvent molecules. Most notably, the solvent has an effect on the four complexes and causes their slight distinctions in the structures. The influence of solvent effect is obviously exhibited in bond distances and angles for complexes **1**, **2**, **3** and **4** (Table 2). Notably, the bond lengths from the O6 atom of coordinated methanol, ethanol, n-propanol or i-propanol molecules to the terminal Ni^{II} ions in complexes **1**, **2**, **3** and **4** are 2.121(3), 2.126(3), 2.118(3) and 2.352(4) Å, respectively, which give a basic regular elongation except n-propanol when the steric hindrance successively becomes larger from methanol, ethanol, n-propanol to i-propanol. Furthermore, in complexes **1**, **2**, **3** and **4**, two imino nitrogen and two phenolic oxygen atoms form the square base with the Ni–N bonds being slightly longer than the corresponding Ni–O bonds. The elongation of the Ni–N bonds is probably owing to the weaker coordination abilities of the nitrogen atoms than of phenolic oxygen atoms. Meanwhile, the angle N1–Ni1–N2 (106.18(16), 99.88(17), 106.24(12) and 98.0(2)°) and O1–Ni1–O4 (79.56(13), 81.13(11), 79.16(9) and 85.73(12)°) formed two imino nitrogen with the terminal Ni^{II} ions as well as two phenolic oxygen atoms with the terminal Ni^{II} ions in Ni^{II} complexes **1**, **2**, **3** and **4** are all different, respectively. That is to say, there is a difference between the degree of distortion of the octahedral geometries of the terminal Ni^{II} ions in complexes **1**, **2**, **3** and **4** because of the solvent effect. In addition, in spite of the supra-molecular structures, complexes **1**, **2**, **3** and **4** also have a similar 0-dimensional structure, which linked by different intra-molecular and/or inter-molecular hydrogen bond interactions. The solvent effects also lead to the changes in UV–Vis, IR spectra, and fluorescence properties in complexes **1**, **2**, **3** and **4**.

4. Conclusions

Four new synthesized Ni^{II} complexes **1**, **2**, **3** and **4** have been designed and characterized structurally. X-ray crystal structure determinations revealed that the structural features of complexes **1**, **2**, **3** and **4** are similar except for the differences in the coordinated and/or crystallizing solvent molecules. They are all tri-nuclear structures with three Ni^{II} ions, two ligand (L)²⁻ moieties, two acetate ligands and two coordinated solvent molecules. Although different solvent molecules are induced in the four Ni^{II} complexes, it is worth noting that all of the Ni^{II} ions in complexes **1**, **2**, **3** and **4** are six-coordinated and possess slightly distorted octahedrons, with different distortion degrees of the octahedral geometries around the Ni^{II} ions. Interestingly, the existence of the solvent effect in complexes **1**, **2**, **3** and **4** may be responsible for the slight differences in their crystal and fluorescence properties. In addition, magnetic susceptibility research performed for complex **2** indicated that the magnetic exchange between the Ni^{II} ions exhibited antiferromagnetic interactions.

Supplementary Materials: The following are available online at <http://www.mdpi.com/2073-4352/8/4/176/s1>, Figure S1: The IR spectra of H₂L and its corresponding Ni^{II} complexes **1**, **2**, **3** and **4**, Table S1: Crystal data and structure refinements for Ni^{II} complexes **2**, **3** and **4**.

Acknowledgments: This work was supported by Program for Excellent Team of Scientific Research in Lanzhou Jiaotong University (201706), which is gratefully acknowledged.

Author Contributions: Yin-Xia Sun conceived and designed the experiments; Jing Li and Hong-Jia Zhang performed the experiments; Jian Chang and Hao-Ran Jia analyzed the data; Yong-Qing Huang contributed analysis tools; Jing Li wrote the paper.

Conflicts of Interest: The authors declare no conflict of interest.

References

1. Sun, S.S.; Stern, C.L.; Nguyen, S.T.; Hupp, J.T. Directed assembly of transition-metal coordinated molecular loops and squares from Salen-type components. Examples of metalation-controlled structural conversion. *J. Am. Chem. Soc.* **2004**, *126*, 6314–6326. [[CrossRef](#)] [[PubMed](#)]
2. Braga, D.; Maini, L.; Polito, M.; Tagliavini, E.; Grepioni, F. Design of hydrogen bonded networks based on organometallic sandwich compounds. *Coord. Chem. Rev.* **2003**, *246*, 53–71. [[CrossRef](#)]
3. Vigato, P.A.; Tamburini, S. Advances in acyclic compartmental ligands and related complexes. *Coord. Chem. Rev.* **2008**, *252*, 1871–1995. [[CrossRef](#)]
4. Song, X.Q.; Lei, Y.K.; Wang, X.R.; Zhao, M.M.; Peng, Y.Q.; Cheng, G.Q. Lanthanide coordination polymers: Synthesis, diverse structure and luminescence properties. *J. Solid State Chem.* **2014**, *218*, 202–212. [[CrossRef](#)]
5. Dong, Y.J.; Dong, X.Y.; Dong, W.K.; Zhang, Y.; Zhang, L.S. Three asymmetric Salamo-type copper(II) and cobalt(II) complexes: Syntheses, structures, fluorescent properties. *Polyhedron* **2017**, *123*, 305–315. [[CrossRef](#)]
6. Zhao, L.; Wang, L.; Sun, Y.X.; Dong, W.K.; Tang, X.L.; Gao, X.H. A supramolecular copper(II) complex bearing Salen-type bisoxime ligand: Synthesis, structural characterization, and thermal property. *Synth. React. Inorg. Met.-Org. Chem.* **2012**, *42*, 1303–1308. [[CrossRef](#)]
7. Zhao, L.; Dong, X.T.; Cheng, Q.; Zhao, J.X.; Wang, L. Synthesis, crystal structure and spectral properties of a 2D supramolecular copper(II) complex with 1-(4-[(E)-3-ethoxyl-2-hydroxybenzylidene]amino}phenyl)ethanone oxime. *Synth. React. Inorg. Met.-Org. Nano-Met. Chem.* **2013**, *43*, 1241–1246. [[CrossRef](#)]
8. Wang, P.; Zhao, L. Synthesis, structure and spectroscopic properties of the trinuclear cobalt(II) and nickel(II) complexes based on 2-hydroxynaphthaldehyde and bis(aminooxy)alkane. *Spectrochim. Acta A* **2015**, *135*, 342–350. [[CrossRef](#)] [[PubMed](#)]
9. Wang, P.; Zhao, L. An infinite 2D supramolecular cobalt(II) complex based on an asymmetric Salamo-type ligand: Synthesis, crystal structure, and spectral properties. *Synth. React. Inorg. Met.-Org. Nano-Met. Chem.* **2016**, *46*, 1095–1101. [[CrossRef](#)]
10. Sun, Y.X.; Wang, L.; Dong, W.K.; Ren, Z.L.; Meng, W.S. Synthesis, characterization, and crystal structure of a supramolecular Co^{II} complex containing Salen-type bisoxime. *Synth. React. Inorg. Met.-Org. Nano-Met. Chem.* **2013**, *43*, 599–603. [[CrossRef](#)]
11. Sun, Y.X.; Zhang, S.T.; Ren, Z.L.; Dong, X.Y.; Wang, L. Synthesis, characterization, and crystal structure of a new supramolecular Cd^{II} complex with halogen-substituted Salen-type bisoxime. *Synth. React. Inorg. Met.-Org. Nano-Met. Chem.* **2013**, *43*, 995–1000. [[CrossRef](#)]
12. Dong, X.Y.; Sun, Y.X.; Wang, L.; Li, L. Synthesis and structure of a penta- and hexa-coordinated tri-nuclear cobalt(II) complex. *J. Chem. Res.* **2012**, *36*, 387–390. [[CrossRef](#)]
13. Sun, Y.X.; Gao, X.H. Synthesis, characterization, and crystal structure of a new Cu^{II} complex with Salen-type ligand. *Synth. React. Inorg. Met.-Org. Nano-Met. Chem.* **2011**, *41*, 973–978. [[CrossRef](#)]
14. Sun, X.Y.; Xu, L.; Zhao, T.H.; Liu, S.H.; Liu, G.H.; Dong, X.T. Synthesis and crystal structure of a 3D supramolecular copper(II) complex with 1-(3-[(E)-3-bromo-5-chloro-2-hydroxybenzylidene]amino}phenyl)ethanone oxime. *Synth. React. Inorg. Met.-Org. Nano-Met. Chem.* **2013**, *43*, 509–513. [[CrossRef](#)]
15. Dong, X.Y.; Akogun, S.F.; Zhou, W.M.; Dong, W.K. Tetranuclear Zn(II) complex based on asymmetrical Salamo-type chelating ligand: Synthesis, structural characterization, and fluorescence property. *J. Chin. Chem. Soc.* **2017**, *64*, 412–419. [[CrossRef](#)]
16. Wu, H.L.; Bai, Y.C.; Zhang, Y.H.; Li, Z.; Wu, M.C.; Chen, C.Y.; Zhang, J.W. Synthesis, crystal structure, antioxidation and DNA-binding properties of a dinuclear copper(II) complex with bis(N-salicylidene)-3-oxapentane-1,5-diamine. *J. Coord. Chem.* **2014**, *67*, 3054–3066. [[CrossRef](#)]
17. Chen, C.Y.; Zhang, J.W.; Zhang, Y.H.; Yang, Z.H.; Wu, H.L.; Pan, G.L.; Bai, Y.C. Gadolinium(III) and dysprosium(III) complexes with a Schiff base bis(N-salicylidene)-3-oxapentane-1,5-diamine: Synthesis, characterization, antioxidation, and DNA-binding studies. *J. Coord. Chem.* **2015**, *68*, 1054–1071. [[CrossRef](#)]

18. Wu, H.L.; Bai, Y.H.; Zhang, Y.H.; Pan, G.L.; Kong, J. Two lanthanide(III) complexes based on the Schiff base *N,N'*-bis(salicylidene)-1,5-diamino-3-oxapentane: Synthesis, characterization, DNA-binding properties, and antioxidation. *Z. Anorg. Allg. Chem.* **2014**, *640*, 2062–2071. [[CrossRef](#)]
19. Wu, H.L.; Pan, G.L.; Bai, C.Y.; Zhang, Y.H.; Wang, H.; Shi, F.R.; Wang, X.L.; Kong, J. Study on synthesis, crystal structure, antioxidant and DNA-binding of mon-, di- and poly-nuclear lanthanides complexes with bis(*N*-salicylidene)-3-oxapentane-1,5-diamine. *J. Photochem. Photobio. B* **2014**, *135*, 33–43. [[CrossRef](#)] [[PubMed](#)]
20. Wu, H.L.; Pan, G.L.; Bai, Y.C.; Wang, H.; Kong, J.; Shi, F.R.; Zhang, Y.H.; Wang, X.L. Preparation, structure, DNA-binding properties, and antioxidant activities of a homodinuclear erbium(III) complex with a pentadentate Schiff base ligand. *J. Chem. Res.* **2014**, *38*, 211–217. [[CrossRef](#)]
21. Wu, H.L.; Wang, C.P.; Wang, F.; Peng, H.P.; Zhang, H.; Bai, Y.C. A new manganese(III) complex from bis(5-methylsalicylaldehyde)-3-oxapentane-1,5-diamine: Synthesis, characterization, antioxidant activity and luminescence. *J. Chin. Chem. Soc.* **2015**, *62*, 1028–1034. [[CrossRef](#)]
22. Wu, H.L.; Wang, H.; Wang, X.L.; Pan, G.L.; Shi, F.R.; Zhang, Y.H.; Bai, Y.C.; Kong, J. V-shaped ligand bis(2-benzimidazolylmethyl)amine containing three copper(II) ternary complexes: Synthesis, structure, DNA-binding properties and antioxidant activity. *New J. Chem.* **2014**, *38*, 1052–1061. [[CrossRef](#)]
23. Wu, H.L.; Pan, G.L.; Bai, Y.C.; Wang, H.; Kong, J.; Shi, F.R.; Zhang, Y.H.; Wang, X.L. A Schiff base bis(*N*-salicylidene)-3-oxapentane-1,5-diamine and its yttrium(III) complex: Synthesis, crystal structure, DNA-binding properties, and antioxidant activities. *J. Coord. Chem.* **2013**, *66*, 2634–2646. [[CrossRef](#)]
24. Wu, H.L.; Pan, G.L.; Bai, Y.C.; Wang, H.; Kong, J.; Shi, F.R.; Zhang, Y.H.; Wang, X.L. Synthesis, structure, antioxidation, and DNA-binding studies of a binuclear ytterbium(III) complex with bis(*N*-salicylidene)-3-oxapentane-1,5-diamine. *Res. Chem. Intermed.* **2015**, *41*, 3375–3388. [[CrossRef](#)]
25. Hu, J.H.; Sun, Y.; Qi, J.; Li, Q.; Wei, T.B. A new unsymmetrical azine derivative based on coumarin group as dual-modal sensor for CN^- and fluorescent “OFF–ON” for Zn^{2+} . *Spectrochim. Acta A* **2017**, *175*, 125–133. [[CrossRef](#)] [[PubMed](#)]
26. H, J.H.; L, J.B.; Q, J.; Chen, J.J. Highly selective and effective mercury(II) fluorescent sensor. *New J. Chem.* **2015**, *39*, 843–848.
27. Dong, W.K.; Akogun, S.F.; Zhang, Y.; Sun, Y.X.; Dong, X.Y. A reversible “turn-on” fluorescent sensor for selective detection of Zn^{2+} . *Sens. Actuators B* **2017**, *238*, 723–734. [[CrossRef](#)]
28. Hu, J.H.; Yan, N.P.; Chen, J.J.; Li, J.B. Synthesis of azosalicylic aldehyde of benzoyl hydrazone based sensor and its colorimetric sensing properties for cyanide anions in aqueous solutions. *Chem. J. Chin. Univ.* **2013**, *34*, 1368–1373.
29. Hu, J.H.; Li, J.B.; Qi, J.; Chen, J.J. Highly selective and elective mercury(II) fluorescent sensors. *New J. Chem.* **2014**, *39*, 843–849. [[CrossRef](#)]
30. Li, J.B.; Hu, J.H.; Chen, J.J.; Qi, J. Cyanide detection using a benzimidazole derivative in aqueous media. *Spectrochim. Acta A* **2014**, *133*, 773–777. [[CrossRef](#)] [[PubMed](#)]
31. Hu, J.H.; Li, J.B.; Qi, J.; Sun, Y. Acylhydrazone based fluorescent chemosensor for zinc in aqueous solution with high selectivity and sensitivity. *Sens. Actuators B* **2015**, *208*, 581–587. [[CrossRef](#)]
32. Sun, Y.; Hu, J.H.; Qi, J.; Li, J.B. A highly selective colorimetric and “turn-on” fluorimetric chemosensor for detecting CN^- based on unsymmetrical azine derivatives in aqueous media. *Spectrochim. Acta A* **2016**, *167*, 101–105. [[CrossRef](#)] [[PubMed](#)]
33. Hu, J.H.; Li, J.B.; Qi, J.; Sun, Y. Selective colorimetric and “turn-on” fluorimetric detection of cyanide using an acylhydrazone sensor in aqueous media. *New J. Chem.* **2015**, *39*, 4041–4046. [[CrossRef](#)]
34. Hu, J.H.; Chen, J.J.; Li, J.B.; Qi, J. A cyanide ion probe based on azosalicylic aldehyde of benzoyl hydrazone. *Chin. J. Inorg. Chem.* **2014**, *30*, 2544–2548.
35. H, J.H.; Li, J.B.; Qi, J.; Sun, Y. Studies on the crystal structure and characterization of *N*-(*acetylphenyl*)-*N'*-(*nitrobenzoyl*)-thiourea. *Phosphorus Sulfur Silicon Relat. Elem.* **2016**, *191*, 984–987.
36. Hu, J.H.; Sun, Y.; Qi, J.; Pei, P.X.; Lin, Q.; Zhang, Y.M. A colorimetric and “turn-on” fluorimetric chemosensor for the selective detection of cyanide and its application in food samples. *RSC Adv.* **2016**, *6*, 100401–100406. [[CrossRef](#)]
37. Hu, J.H.; Yan, N.P.; Chen, J.J. Synthesis of 4–nitrophenylthiosemicarbazone of salicylaldehyde and its colorimetric anion recognition properties. *J. Chem. Res.* **2012**, *36*, 619–622. [[CrossRef](#)]

38. Dong, W.K.; Ma, J.C.; Dong, Y.J.; Zhu, L.C.; Zhang, Y. Di- and tetranuclear heterometallic 3d–4f cobalt(II)–lanthanide(III) complexes derived from a hexadentate bisoxime: Syntheses, structures and magnetic properties. *Polyhedron* **2016**, *115*, 228–235. [[CrossRef](#)]
39. Song, X.Q.; Zheng, Q.F.; Wang, L.; Liu, W.S. Synthesis and luminescence properties of lanthanide complexes with a new tripodal ligand featuring *N*-thenylsalicylamide arms. *Luminescence* **2012**, *27*, 459–465. [[CrossRef](#)] [[PubMed](#)]
40. Zhang, H.; Dong, W.K.; Zhang, Y.; Akogun, S.F. Naphthalenediol-based bis(Salamo)-type homo- and heterotrinnuclear cobalt(II) complexes: Syntheses, structures and magnetic properties. *Polyhedron* **2017**, *133*, 279–293. [[CrossRef](#)]
41. Liu, P.P.; Sheng, L.; Song, X.Q.; Xu, W.Y.; Liu, Y.A. Synthesis, structure and magnetic properties of a new one dimensional manganese coordination polymer constructed by a new asymmetrical ligand. *Inorg. Chim. Acta* **2015**, *434*, 252–257. [[CrossRef](#)]
42. Song, X.Q.; Liu, P.P.; Xiao, Z.R.; Li, X.; Liu, Y.A. Four polynuclear complexes based on a versatile salicylamide salen-like ligand: Synthesis, structural variations and magnetic properties. *Inorg. Chim. Acta* **2015**, *438*, 232–244. [[CrossRef](#)]
43. Song, X.Q.; Peng, Y.J.; Chen, G.Q.; Wang, X.R.; Liu, P.P.; Xu, W.Y. Substituted group-directed assembly of Zn(II) coordination complexes based on two new structural related pyrazolone based Salen ligands: Syntheses, structures and fluorescence properties. *Inorg. Chim. Acta* **2015**, *427*, 13–21. [[CrossRef](#)]
44. Song, X.Q.; Cheng, G.Q.; Wang, X.R.; Xu, W.Y.; Liu, P.P. Structure-based description of a step-by-step synthesis of heterodinuclear Zn^{II}Ln^{III} complexes and their luminescence properties. *Inorg. Chim. Acta* **2015**, *425*, 145–153. [[CrossRef](#)]
45. Song, X.Q.; Liu, P.P.; Liu, Y.A.; Zhou, J.J.; Wang, X.L. Two dodecanuclear heterometallic [Zn₆Ln₆] clusters constructed by a multidentate salicyl-amide salen-like ligand: Synthesis, structure, luminescence and magnetic properties. *Dalton Trans.* **2016**, *45*, 8154–8163. [[CrossRef](#)] [[PubMed](#)]
46. Song, X.Q.; Wang, L.; Zheng, Q.F.; Liu, W.S. Synthesis, crystal structure and luminescence properties of lanthanide complexes with a new semirigid bridging furfuryl salicylamide ligand. *Inorg. Chim. Acta* **2012**, *391*, 171–178. [[CrossRef](#)]
47. Zheng, S.S.; Dong, W.K.; Zhang, Y.; Chen, L.; Dong, Y.G. Four Salamo-type 3d–4f hetero-bimetallic [Zn^{II}Ln^{III}] complexes: Syntheses, crystal structures, and luminescent and magnetic properties. *New J. Chem.* **2017**, *41*, 4966–4973. [[CrossRef](#)]
48. Dong, X.Y.; Kang, Q.P.; Jin, B.X.; Dong, W.K. A dinuclear nickel(II) complex derived from an asymmetric Salamo-type N₂O₂ chelate ligand: Synthesis, structure and optical properties. *Z. Naturforsch.* **2017**, *72*, 415–420. [[CrossRef](#)]
49. Dong, W.K.; Zhu, L.C.; Ma, J.C.; Sun, Y.X.; Zhang, Y. Two novel mono- and heptanuclear Ni(II) complexes constructed from new unsymmetric and symmetric Salamo-type bisoximes – Synthetic, structural and spectral studies. *Inorg. Chim. Acta* **2016**, *453*, 402–408. [[CrossRef](#)]
50. Liu, P.P.; Wang, C.Y.; Zhang, M.; Song, X.Q. Pentanuclear sandwich-type Zn^{II}-Ln^{III} clusters based on a new Salen-like salicylamide ligand: Structure, near-infrared emission and magnetic properties. *Polyhedron* **2017**, *129*, 133–140. [[CrossRef](#)]
51. Dong, W.K.; Ma, J.C.; Zhu, L.C.; Zhang, Y. Nine self-assembled nickel(II)–lanthanide(III) heterometallic complexes constructed from a Salamo-type bisoxime and bearing N- or O-donor auxiliary ligand: Syntheses, structures and magnetic properties. *New J. Chem.* **2016**, *40*, 6998–7010. [[CrossRef](#)]
52. Chen, L.; Dong, W.K.; Zhang, H.; Zhang, Y.; Sun, Y.X. Structural Variation and Luminescence Properties of Tri- and Dinuclear CuII and ZnII Complexes Constructed from a Naphthalenediol-Based Bis(Salamo)-type Ligand. *Cryst. Growth Des.* **2017**, *17*, 3636–3648. [[CrossRef](#)]
53. Chai, L.Q.; Wang, G.; Sun, Y.X.; Dong, W.K.; Zhao, L.; Gao, X.H. Synthesis, crystal structure, and fluorescence of an unexpected dialkoxo-bridged dinuclear copper(II) complex with bis(salen)-type tetraoxime. *J. Coord. Chem.* **2012**, *65*, 1621–1631. [[CrossRef](#)]
54. Chai, L.Q.; Huang, J.J.; Zhang, H.S.; Zhang, Y.L.; Zhang, J.Y.; Li, Y.X. An unexpected cobalt(III) complex containing a Schiff base ligand: Synthesis, crystal structure, spectroscopic behavior, electrochemical property and SOD-like activity. *Spectrochim. Acta A* **2014**, *131*, 526–533. [[CrossRef](#)] [[PubMed](#)]

55. Chai, L.Q.; Liu, G.; Zhang, J.Y.; Huang, J.J.; Tong, J.F. Synthesis, crystal structure, fluorescence, electrochemical property, and SOD-like activity of an unexpected nickel(II) complex with a quinazoline-type ligand. *J. Coord. Chem.* **2013**, *66*, 3926–3938. [[CrossRef](#)]
56. Chai, L.Q.; Zhang, H.S.; Huang, J.J.; Zhang, Y.L. An unexpected Schiff base-type Ni(II) complex: Synthesis, crystal structures, fluorescence, electrochemical property and SOD-like activities. *Spectrochim. Acta A* **2015**, *137*, 661–669. [[CrossRef](#)] [[PubMed](#)]
57. Chai, L.Q.; Tang, L.J.; Chen, L.C.; Huang, J.J. Structural, spectral, electrochemical and DFT studies of two mononuclear manganese(II) and zinc(II) complexes. *Polyhedron* **2017**, *122*, 228–240. [[CrossRef](#)]
58. Li, G.; Hao, J.; Liu, L.Z.; Zhou, W.M.; Dong, W.K. Syntheses, Crystal Structures and Thermal Behaviors of Two Supramolecular Salamo-Type Cobalt(II) and Zinc(II) Complexes. *Crystals* **2017**, *7*, 217.
59. Xu, L.; Zhu, L.C.; Ma, J.C.; Zhang, Y.; Dong, W.K. Syntheses, structures and spectral properties of mononuclear Cu^{II} and dimeric Zn^{II} complexes based on an asymmetric Salamo-type N₂O₂ ligand. *Z. Anorg. Allg. Chem.* **2015**, *641*, 2520–2524. [[CrossRef](#)]
60. Yang, Y.H.; Hao, J.; Dong, Y.J.; Wang, G.; Dong, W.K. Two Zinc(II) Complexes Constructed from a Bis(salamo)-type Tetraoxime Ligand: Syntheses, Crystal Structures and Luminescence Properties. *Chin. J. Inorg. Chem.* **2017**, *33*, 1280–1292.
61. Chai, L.Q.; Zhang, K.Y.; Tang, L.J.; Zhang, J.Y.; Zhang, H.S. Two mono- and dinuclear Ni(II) complexes constructed from quinazoline-type ligands: Synthesis, X-ray structures, spectroscopic, electrochemical, thermal, and antimicrobial studies. *Polyhedron* **2017**, *130*, 100–107. [[CrossRef](#)]
62. Dong, X.Y.; Kang, Q.P.; Li, X.Y.; Ma, J.C.; Dong, W.K. Structurally characterized solvent-induced homotrimeric cobalt(II) N₂O₂-donor bisoxime-type complexes. *Crystals* **2018**, *8*, 139.
63. Dong, X.Y.; Li, X.Y.; Liu, L.Z.; Zhang, H.; Ding, Y.J.; Dong, W.K. Tri- and hexanuclear heterometallic Ni(II)–M(II) (M=Ca, Sr and Ba) bis(salamo)-type complexes: synthesis, structure and fluorescence properties. *RSC Adv.* **2017**, *7*, 48394–48403. [[CrossRef](#)]
64. Wang, L.; Li, X.Y.; Zhao, Q.; Li, L.H.; Dong, W.K. Fluorescence properties of heterotrimeric Zn(II)–M(II) (M=Ca, Sr and Ba) bis(salamo)-type complexes. *RSC Adv.* **2017**, *7*, 48730–48737. [[CrossRef](#)]
65. Dong, W.K.; Ma, J.C.; Zhu, L.C.; Zhang, Y.; Li, X.L. Four new nickel(II) complexes based on an asymmetric Salamo-type ligand: Synthesis, structure, solvent effect and electrochemical property. *Inorg. Chim. Acta* **2016**, *445*, 140–148. [[CrossRef](#)]
66. Dong, W.K.; Du, W.; Zhang, X.Y.; Li, G.; Dong, X.Y. Synthesis, crystal structure and spectral properties of a supramolecular trinuclear nickel(II) complex with 5-methoxy-4'-bromo-2,2'-[ethylenedioxybis(nitrilomethylidyne)]diphenol. *Spectrochim. Acta A* **2014**, *132*, 588–593. [[CrossRef](#)] [[PubMed](#)]
67. Dong, W.K.; Sun, Y.X.; Li, L.; Zhang, S.T.; Wang, L.; Dong, X.Y.; Gao, X.H. A tetradentate bisoxime and its supramolecular nickel(II) cluster: Synthesis, crystal structure, and spectral properties. *J. Coord. Chem.* **2012**, *65*, 2332–2340. [[CrossRef](#)]
68. Dong, W.K.; Sun, Y.X.; Zhao, C.Y.; Dong, X.Y.; Xu, L. Synthesis, structure and properties of supramolecular Mn^{II}, Co^{II}, Ni^{II} and Zn^{II} complexes containing Salen-type bisoxime ligands. *Polyhedron* **2010**, *29*, 2087–2097. [[CrossRef](#)]
69. Liu, Y.A.; Wang, C.Y.; Zhang, M.; Song, X.Q. Structures and magnetic properties of cyclic heterometallic tetranuclear clusters. *Polyhedron* **2017**, *127*, 278–286. [[CrossRef](#)]
70. Jeon, Y.-M.; Heo, J.; Mirkin, C.A. Acid-functionalized dissymmetric salen ligands and their manganese(III) complexes. *Tetrahed. Lett.* **2007**, *48*, 2591–2595. [[CrossRef](#)]
71. Dong, W.K.; Xing, S.J.; Sun, Y.X.; Zhao, L.; Chai, L.Q.; Gao, X.H. An unprecedented tetranuclear Zn(II) complex with an unsymmetric Salen-type bisoxime ligand: Synthesis, crystal structure, and spectral properties. *J. Coord. Chem.* **2012**, *65*, 1212–1220. [[CrossRef](#)]
72. Ren, Z.L.; Wang, F.; Liu, L.Z.; Jin, B.X.; Dong, W.K. Unprecedented hexanuclear cobalt(II) nonsymmetrical salamo-Based coordination compound: synthesis, crystal structure, and photophysical properties. *Crystals* **2018**, *8*, 144.
73. Dong, W.K.; Zhu, L.C.; Dong, Y.J.; Ma, J.C.; Zhang, Y. Mono, di and heptanuclear metal(II) complexes based on symmetric and asymmetric tetradentate Salamo-type ligands: Syntheses, structures and spectroscopic properties. *Polyhedron* **2016**, *117*, 148–154. [[CrossRef](#)]

74. Dong, W.K.; Zhang, J.T.; Dong, Y.J.; Zhang, Y.; Wang, Z.K. Construction of mononuclear copper(II) and trinuclear cobalt(II) complexes based on asymmetric Salamo-type ligands. *Z. Anorg. Allg. Chem.* **2016**, *642*, 189–196. [[CrossRef](#)]
75. Dong, W.K.; Zhang, J.; Zhang, Y.; Li, N. Novel multinuclear transition metal(II) complexes based on an asymmetric Salamo-type ligand: Syntheses, structure characterizations and fluorescent properties. *Inorg. Chim. Acta* **2016**, *444*, 95–102. [[CrossRef](#)]
76. Kim, G.J.; Shin, J.H. Application of new unsymmetrical chiral Mn(III), Co(II,III) and Ti(IV) salen complexes in enantioselective catalytic reactions. *Catal. Lett.* **1999**, *63*, 83–90. [[CrossRef](#)]
77. Dong, W.K.; Sun, Y.X.; Liu, G.H.; Li, L.; Dong, X.Y.; Gao, X.H. Two supramolecular nickel(II) complexes: Syntheses, crystal structures and solvent effects. *Z. Anorg. Allg. Chem.* **2012**, *638*, 1370–1377. [[CrossRef](#)]
78. Dong, W.K.; Wang, G.; Gong, S.S.; Tong, J.F.; Sun, Y.X.; Gao, X.H. Synthesis, structural characterization and substituent effects of two copper(II) complexes with benzaldehyde ortho-oxime ligands. *Transit. Met. Chem.* **2012**, *37*, 271–277. [[CrossRef](#)]
79. Dong, W.K.; Tong, J.F.; Sun, Y.X.; Wu, J.C.; Yao, J.; Gong, S.S. Studies on mono- and dinuclear bisoxime copper complexes with different coordination geometries. *Transit. Met. Chem.* **2010**, *35*, 419–426. [[CrossRef](#)]
80. Dong, W.K.; Lan, P.F.; Zhou, W.M.; Zhang, Y. Salamo-type trinuclear and tetranuclear cobalt(II) complexes based on a new asymmetry Salamo-type ligand: Syntheses, crystal structures, and fluorescence properties. *J. Coord. Chem.* **2016**, *69*, 1272–1283. [[CrossRef](#)]
81. Dong, W.K.; Chen, X.; Sun, Y.X.; Yang, Y.H.; Zhao, L.; Xu, L.; Yu, T.Z. Synthesis, structure and spectroscopic properties of two new trinuclear nickel(II) clusters possessing solvent effect. *Spectrochim. Acta A* **2009**, *74*, 719–725. [[CrossRef](#)] [[PubMed](#)]
82. Dong, W.K.; He, X.N.; Yan, H.B.; Lv, Z.W.; Chen, X.; Zhao, C.Y.; Tang, X.L. Synthesis, structural characterization and solvent effect of copper(II) complexes with a variational multidentate Salen-type ligand with bisoxime groups. *Polyhedron* **2009**, *28*, 1419–1428. [[CrossRef](#)]
83. Sun, Y.X.; Li, C.Y.; Yang, C.J.; Zhao, Y.Y.; Guo, J.Q.; Yu, B. Two Cu(II) complexes with Schiff base ligands: Syntheses, crystal structures, spectroscopic properties, and substituent effect. *Chin. J. Inorg. Chem.* **2016**, *32*, 327–335.
84. Dong, W.K.; Zhang, F.; Li, N.; Xu, L.; Zhang, Y.; Zhang, J.; Zhu, L.C. Trinuclear cobalt(II) and zinc(II) salamo-type complexes: Syntheses, crystal structures, and fluorescent properties. *Z. Anorg. Allg. Chem.* **2016**, *642*, 532–538. [[CrossRef](#)]
85. Dong, W.K.; Li, X.L.; Wang, L.; Zhang, Y.; Ding, Y.J. A new application of Salamo-type bisoximes: As a relay-sensor for Zn²⁺/Cu²⁺ and its novel complexes for successive sensing of H⁺/OH⁻. *Sens. Actuators B* **2016**, *229*, 370–378. [[CrossRef](#)]
86. Dong, W.K.; Guan, Y.H.; Shi, J.Y.; Zhao, C.Y. Synthesis, crystal structure and spectroscopic behaviors of Co(II) and Cu(II) complexes with Salen-type bisoxime ligands. *Inorg. Chim. Acta* **2009**, *362*, 1129–1134. [[CrossRef](#)]
87. Dong, W.K.; Sun, Y.X.; Zhang, Y.P.; Li, L.; He, X.N.; Tang, X.L. Synthesis, crystal structure, and properties of supramolecular Cu^{II}, Zn^{II}, and Cd^{II} complexes with Salen-type bisoxime ligands. *Inorg. Chim. Acta* **2009**, *362*, 117–124. [[CrossRef](#)]
88. Dong, W.K.; Ma, J.C.; Zhu, L.C.; Sun, Y.X.; Akogun, S.F.; Zhang, Y. A Series of heteromultinuclear zinc(II)–lanthanide(III) complexes based on 3-MeOsalamo: Syntheses, structural characterizations, and luminescent properties. *Cryst. Growth Des.* **2016**, *16*, 6903–6914. [[CrossRef](#)]
89. Gao, L.; Wang, F.; Zhao, Q.; Zhang, Y.; Dong, W.K. Mononuclear Zn(II) and trinuclear Ni(II) complexes derived from a coumarin-containing N₂O₂ ligand: Syntheses, crystal structures and fluorescence properties. *Polyhedron* **2018**, *139*, 7–16. [[CrossRef](#)]
90. Majumder, A.; Rosair, G.M.; Mallick, A.; Chattopadhyay, N.; Mitra, S. Synthesis, structures and fluorescence of nickel, zinc and cadmium complexes with the N,N,O-tridentate Schiff base N-2-pyridylmethylidene-2-hydroxy-phenylamine. *Polyhedron* **2006**, *25*, 1753–1762. [[CrossRef](#)]

91. Ghosh, T.; Mondal, B.; Ghosh, T.; Sutradhar, M.; Mukherjee, G.; Drew, M.G.B. Synthesis, structure, solution chemistry and the electronic effect of para substituents on the vanadium center in a family of mixed-ligand [(VO)-O-V(ONO)(ON)] complexes. *Inorg. Chim. Acta* **2007**, *360*, 1753–1761. [[CrossRef](#)]
92. Qi, J.; Wang, Q.L.; Zhang, A.P.; Tian, J.L.; Yan, S.P.; Cheng, P.; Yang, G.M.; Liao, D.Z. Synthesis, crystal structure, spectroscopy and magnetism of a trinuclear nickel(II) complex with 3,5-pyrazoledicarboxylic acid as bridge ligands. *C. R. Chim* **2014**, *17*, 490–495. [[CrossRef](#)]



© 2018 by the authors. Licensee MDPI, Basel, Switzerland. This article is an open access article distributed under the terms and conditions of the Creative Commons Attribution (CC BY) license (<http://creativecommons.org/licenses/by/4.0/>).